# Myeloperoxidase-induced Genomic DNA-centered Radicals*

**Sandra E. Gomez-Mejiba**[‡1], **Zili Zhai**[‡], **Maria S. Gimenez**[§], **Michael T. Ashby**[¶], **Jaya Chilakapati**[‖], **Kirk Kitchin**[‖], **Ronald P. Mason**[**2], and **Dario C. Ramirez**[‡3]

From the [‡]*Experimental Therapeutics Research Program, Oklahoma Medical Research Foundation, Oklahoma City, Oklahoma 73104,* [§]*Instituto Multidisciplinario de Investigaciones Biológicas, Consejo Nacional de Investigaciones Científicas y Técnicas, Universidad Nacional de San Luis, San Luis 5700, Argentina, the* [¶]*Department of Chemistry and Biochemistry, University of Oklahoma, Norman, Oklahoma 73019, and the* [‖]*Integrated Systems Toxicology Division, National Health and Environmental Effects Research Laboratory, United States Environmental Protection Agency, and the* [**]*Laboratory of Pharmacology, NIEHS, National Institutes of Health, Research Triangle Park, North Carolina 27709*

**Myeloperoxidase (MPO) released by activated neutrophils can initiate and promote carcinogenesis. MPO produces hypochlorous acid (HOCl) that oxidizes the genomic DNA in inflammatory cells as well as in surrounding epithelial cells. DNA-centered radicals are early intermediates formed during DNA oxidation. Once formed, DNA-centered radicals decay by mechanisms that are not completely understood, producing a number of oxidation products that are studied as markers of DNA oxidation. In this study we employed the 5,5-dimethyl-1-pyrroline *N*-oxide-based immuno-spin trapping technique to investigate the MPO-triggered formation of DNA-centered radicals in inflammatory and epithelial cells and to test whether resveratrol blocks HOCl-induced DNA-centered radical formation in these cells. We found that HOCl added exogenously or generated intracellularly by MPO that has been taken up by the cell or by MPO newly synthesized produces DNA-centered radicals inside cells. We also found that resveratrol passed across cell membranes and scavenged HOCl before it reacted with the genomic DNA, thus blocking DNA-centered radical formation. Taken together our results indicate that the formation of DNA-centered radicals by intracellular MPO may be a useful point of therapeutic intervention in inflammation-induced carcinogenesis.**

Activation of neutrophils can initiate chemical mutagenesis and carcinogenesis by producing oxidative damage to the genome in the inflammatory environment (1–3). Myeloperoxidase (MPO,[4] donor hydrogen peroxide, oxidoreductase, EC 1.11.1.7), is a hemeprotein found in the azurophilic granules of

neutrophils (4–6). MPO uses $H_2O_2$ to oxidize chloride ions, converting them into the powerful oxidant hypochlorous acid (HOCl/OCl⁻, p$K_a$ = 7.46) (5). Although other mammalian peroxidases can oxidize a number of halides and pseudohalides to hypohalous and pseudohypohalous acids, MPO is the only mammalian enzyme that produces HOCl under physiological conditions (5). In sites of inflammation, $H_2O_2$ used in the MPO-catalyzed oxidation of chloride is produced by dismutation of superoxide radical anion ($O_2^-$). It is noteworthy that DNA is negatively charged and MPO is a cationic protein (5), which suggests that they can bind each other by electrostatic interactions. MPO is known to be taken up by cells surrounding an inflammatory site (7). It might be anticipated that this would make them highly vulnerable to DNA damage induced by $H_2O_2$.

DNA-chloramines, which are less reactive than HOCl, are produced when HOCl reacts with DNA at its heterocyclic (ring) amino groups of guanosine and thymine groups and with exocyclic amino groups of guanosine, adenosine, and cytidine (8). Once formed, DNA-chloramines appear to undergo both one- and two-electron decay to produce DNA nitrogen-centered radicals, a process that is catalyzed by reduced metals and is promoted by UV irradiation and high temperatures (8–9). Importantly, nitrogen- and carbon-centered radicals can be trapped by 5,5-dimethyl-1-pyrroline *N*-oxide (DMPO) to form radical adducts, which in the case of DNA then decay to form DNA-DMPO nitrone adducts (referred to as DNA nitrone adducts or nitrone adducts). Herein, we studied the DNA nitrone adducts using DMPO-based immuno-spin trapping that employs an anti-DMPO antibody (10, 11).

Resveratrol (*trans*-3,5,4′-trihydroxy-*trans*-stilbene) is a naturally occurring compound that has been shown to prevent some forms of cancer (12–14) and other inflammatory diseases (15, 16); however, the mechanism of action remains to be elucidated. Notably, resveratrol has been shown to inhibit the peroxidase activity of MPO (17); however, no studies have been published regarding its ability to scavenge HOCl.

In this study we used DMPO-based immuno-spin trapping to investigate the formation of DNA-centered radicals in cells. We have focused the present study on the generation of DNA-

centered radicals by HOCl produced by MPO. We studied the ability of MPO taken up by epithelial cells or MPO contained/synthesized inside inflammatory cells to produce DNA-centered radicals when exposed to $H_2O_2$. We also tested whether resveratrol prevents DNA oxidation by HOCl produced exogenously or intracellularly. We found that DNA-centered radicals are formed when HOCl is produced by MPO in close proximity to the nucleus. We also showed that resveratrol passes across membranes, scavenges HOCl, and thus, blocks genomic DNA-centered radical formation in cells. Our results suggest a mechanism of MPO-driven, HOCl-triggered early events in oxidatively generated damage to the genome and provide a new point of potential intervention in inflammation-induced carcinogenesis.

## EXPERIMENTAL PROCEDURES

*Reagents*—Calf thymus double-stranded deoxyribonucleic acid (dsDNA, ~10,000–15,000 kDa) as its sodium salt (catalog #D3664, lot #015K7019), glucose oxidase from buttermilk (GO), D-glucose, phorbol 12-myristate 13-acetate (PMA), taurine, reduced glutathione (GSH), L-ascorbate, diphenylene iodonium, and hypochlorous acid (HOCl, 30%) were obtained from Sigma. Apocynin and 4-aminobenzoic acid hydrazide (ABAH) were from Calbiochem. Stock solutions of HOCl were prepared in 10 mM NaOH (pH ~ 12), and its molar concentration was calculated using a molar coefficient at 292 nm, $\epsilon_{292} = 350$ M$^{-1}$ cm$^{-1}$. HOCl bolus solutions were prepared at concentrations 100 times higher than that required in the final reaction to avoid change in the final pH of the reaction mixture, typically 7.4. Human MPO and the anti-human MPO antibody were purchased from Athens Research and Technology (Atlanta, GA). Human leukemia (HL)-60 cells, RAW 264.7 murine macrophages, and A549 human type II airway epithelial cells were purchased from American Tissue Cell Collection (Manassas, VA) and maintained as indicated by the product's instructions. The nitrone spin trap DMPO ($\epsilon_{228} = 7800$ M$^{-1}$ cm$^{-1}$) and the anti-DMPO serum were purchased from Alexis Biochemicals (San Diego, CA) and kept stored in aliquots at −80 °C until use. Reagent grade 30% $H_2O_2$ ($\epsilon_{240} = 43.6$ M$^{-1}$ cm$^{-1}$) was from Fisher Scientific Co. (Fair Lawn, NJ). All buffers used in our experiments were treated with Chelex® 100 ion exchange resin (Bio-Rad) to remove transition metals usually found in phosphate buffers as contaminants.

*DNA Preparation and Production of HOCl-induced DNA-DMPO Nitrone Adducts*—A stock solution of calf thymus DNA was prepared as previously described (18). The concentration of DNA was calculated from its absorbance at 260 nm ($A_{260 nm} = 1$ corresponds to ~50 $\mu$g/ml dsDNA ~ 150 $\mu$M as bases). Typically, 5 $\mu$M DNA (as bases) were reacted in a total volume of 300 $\mu$l with 10 $\mu$M HOCl in 100 mM Chelex sodium phosphate (NaP) buffer at pH 7.4 and 37 °C for 15 min followed by the addition of 10 mM DMPO. Thirty minutes later the reaction was stopped by adding 3 $\mu$l of a 1 M solution of methionine in 0.1 M HCl to scavenge excess HOCl and reactive chloramines (19).

*Luminol-based Assay of HOCl and Study of Scavengers*—Under our experimental conditions luminol reacts with HOCl to produce luminescence but not with $H_2O_2$, $O_2^-$ produced from acetaldehyde/xanthine or peroxynitrite produced from 3-morpholinosydnonimine *N*-ethylcarbamide (SIN-1) decomposition. These observations are in agreement with a recent study which showed that luminol is a specific probe for imaging HOCl produced by MPO *in vivo* (20). Fifty $\mu$l of 10 $\mu$M luminol were, therefore, mixed in each well of a 96-well black microplate with an equal volume of resveratrol dissolved in 100 mM Chelex-NaP buffer, pH 7.4. The reaction was started by adding 100 $\mu$l of 100 mM NaP buffer with 100 $\mu$M HOCl, and the luminescence was read in a microplate reader within 2 min of mixing the reagents at 15–22 °C.

*Preparation of MPO*—100 $\mu$g of MPO were dissolved in 200 $\mu$l of ultrapure water and dialyzed overnight against 2 liters of 10 mM Chelex-NaP buffer, pH 7.4, using a Dialyzer cassette with a 5-kDa cut-off (Pierce). Before the addition of MPO to cell culture medium, the solution was sterilized by passing it through a 0.22-$\mu$m nylon syringe filter. The UV-visible spectrum was used to determine the concentration, identity, and purity of the MPO. The Soret band with a peak maximum at 430 nm (178,000 M$^{-1}$ cm$^{-1}$ for the MPO homodimer at pH 7.4) is characteristic of the specific heme prosthetic group in MPO. The rheinheitzahl value ($A_{430}/A_{280}$ ratio) from the UV-visible spectra provided an estimate of the purity of MPO relative to total protein. The preparations of MPO used in our experiments had a rheinheitzahl value of 0.8 (5).

*Assay of the Peroxidase Activity of MPO*—The peroxidase activity of MPO was measured after the $H_2O_2$-catalyzed oxidation of guaiacol to tetraguaiacol at 15–22 °C. Typically, the reaction mixture contained 8.9 mM guaiacol, 50 nM MPO in 500 $\mu$l of a 50 mM acetic acid/acetate buffer, pH 5.6. The reaction was started by adding different concentrations of $H_2O_2$, and the formation of tetraguaiacol at 470 nm ($\epsilon_{470 nm} = 26.6$ mM$^{-1}$ cm$^{-1}$) was quantified within the first minute of reaction.

*Production of DNA-DMPO Nitrone Adducts Using the MPO/$H_2O_2$/$Cl^-$ System*—Typically, 5 $\mu$M calf thymus DNA solution, 2 nM MPO, and 3 $\mu$l of an $H_2O_2$ solution 100 times more concentrated than that required to reach the final concentration, stated in each experiment, were reacted in 300 $\mu$l of 10 mM Chelex-NaP buffer containing 100 mM NaCl at pH 7.4. The reaction mixture was incubated at 37 °C and at 700 rpm in a thermomixer. In experiments where $H_2O_2$ was produced by the glucose/GO system, the buffer contained 5.6 mM $\beta$-D-glucose, and an appropriate volume to obtain the final required concentration of GO was added from a 100× stock solution. Thirty minutes after the addition of the bolus $H_2O_2$ or after initiation of $H_2O_2$ generation by the addition of GO, 10 mM DMPO was added, and the incubation was continued for an additional 30 min. The reaction was terminated with 10 mM methionine that scavenges the HOCl excess or by adding 10 mM KCN to inhibit MPO activity. To decompose $H_2O_2$ produced by the glucose/GO system, 2 IU/ml catalase was added.

*Induction and Visualization of DNA Nitrone Adducts Inside HL-60 Cells*—The HL-60 cell line was kept in RPMI 1640 medium containing 10% fetal calf serum. Before use the HL-60 cells were collected by centrifugation at 200 × $g$ for 5 min at 4 °C. The cells were washed 3 times with sterile calcium-magnesium-free Hanks'-buffered saline solution (HBSS$^-$) and resuspended to obtain a suspension of $10^7$ cells in 500 $\mu$l of 10 mM

## HOCl-triggered DNA-centered Radicals in Cells

Chelex-NaP buffer with 100 mM sodium chloride at pH 7.4. It should be noted that the intracellular concentration of $Cl^-$ is 25 times lower than the extracellular fluids, *i.e.* ~4 mM. The formation of HOCl was started by adding a bolus of $H_2O_2$ or by adding 1–5 milli-IU of GO from a 100× stock solution. After 30 min of incubation at 37 °C, 10 mM DMPO was added, and the incubation was continued for 30 min more at 37 °C. The reaction was stopped with 5 μl of a solution containing 200 IU catalase, 100 mM DTPA, 1 M methionine in NaP buffer and by washing the cells 3 times with 1 ml of PBS containing 10 mM methionine. Cell viability was then measured in one aliquot using the trypan blue exclusion assay. Another aliquot of cells was used to prepare cytospin slides for immunostaining of DNA-DMPO nitrone adducts. The remaining cells were pelleted and frozen and stored at −80 °C until DNA extraction and analysis of DNA-DMPO nitrone adducts.

The subcellular distribution of nitrone adducts in cytospin preparations of HL-60 cells was determined by laser-scanning confocal microscopy. Briefly, for the cytospin preparation, the cell suspension was diluted to $10^4$ cells/ml in PBS. Then, a total volume of 700 μl of cell suspension was centrifuged ($700 \times g$, 10 min) in a Shadon 4 cytospin centrifuge (Thermo Fisher Scientific). After that, the slide was rinsed with PBS, fixed with 4% paraformaldehyde for 15 min at 37 °C, and then permeabilized with 0.2% Triton X-100 at room temperature for 5 min followed by blocking with the Image-iT™ FX signal enhancer (Invitrogen) for 30 min at 15–22 °C. The fixed cells were incubated overnight at 4 °C with the rabbit anti-DMPO (1:500 dilution in PBS), washed, and then incubated with a goat anti-rabbit Alexa Fluor 488 (1:1000) at 37 °C for 1 h. Finally, the slides were washed with PBS and mounted using Prolong Gold anti-fade reagent with 4,6-diamino-2-phenylindole (Invitrogen), and the preparation was examined with a Leica SP2 MP Confocal Microscope with a 63 × 1.4 oil immersion objective. Single plane images were acquired and analyzed using LSM 5 image examiner software.

*Induction of MPO in Macrophages with Lipopolysaccharide (LPS) and Activation with PMA*—The synthesis of MPO by RAW 264.7 macrophages (80% coverage in T-75 flasks) was induced with 1 ng/ml bacterial endotoxin (LPS, *Escherichia coli*, serotype 055:B5) in phenol-red free-Dulbecco's modified Eagle's medium containing 5% fetal calf serum for 24 h. A parallel experiment was run to obtain a macrophage homogenate for analyzing MPO protein by Western blot. After exposure to LPS, the macrophage monolayers were rinsed twice with pre-warmed HBSS containing calcium and magnesium ($HBSS^+$) followed by the addition of 1 ng/ml PMA for 1 h, and then DMPO was added to the medium at a final concentration of 50 mM. Incubation was continued for 1 h after the addition of the DMPO. After completion of the incubation, the medium was removed, the monolayer was washed with $HBSS^-$, and the cells were harvested by scraping, washed, and frozen for further DNA extraction and analysis of DNA-DMPO nitrone adducts.

*Pre-loading of A549 Cells with Human MPO and Induction of DNA-centered Radicals*—A549 human type II airway epithelial cells were cultured in F12K medium containing 5% fetal calf serum in T-75 flasks up to 90% coverage or cultured $10^5$ cells/ml in an 8-well LabTek glass slide. The monolayers were rinsed with $HBSS^+$ and incubated in F12K medium with 5% fetal calf serum containing 10 nM human MPO for 24 h. The medium was then removed, and the monolayers were rinsed three times with pre-warmed $HBSS^+$. In the cells loaded with MPO and grown in T-75 flasks, the production of HOCl was initiated by adding different concentrations of GO in $HBSS^+$ containing 5.6 mM glucose to produce $H_2O_2$. Typically, the formation of $H_2O_2$ was started with GO and incubating the monolayer for 30 min followed by the addition of 25 mM DMPO. One h later the medium was removed, the monolayer was rinsed, and the cells were harvested for analysis of viability using trypan blue and DNA extraction. A LabTek glass slide that was treated in a similar way was used to localize the uptaken MPO using immunocytochemistry. After the inhibition of the endogenous peroxidases activity with 10 mM KCN, the slide was blocked and incubated with an anti-human MPO antibody/horseradish peroxidase-conjugated secondary antibody, and the immuno-complexes were developed with a diaminobenzidine substrate kit (Pierce). The image was acquired at 400× magnification using a Jenco inverted digital microscope.

*DNA Extraction and Analysis of DNA-DMPO Nitrone Adducts*—The extraction of DNA using a chloroform-phenol-based procedure and further analysis of DNA-DMPO nitrone adducts by ELISA with the anti-DMPO antibody were previously reported (18).

*Isolation of Neutrophils and Co-culture with A549 Cells*—Human neutrophils were isolated from venous blood by buoyant density centrifugation (21), and their purity was determined by analysis of a cytospin slide stained with Diff-Quick (Thermo Fisher Scientific). Confluent monolayers of A549 cells, $10^6$ isolated human neutrophils, or both in co-culture were incubated in 2 ml of $HBSS^+$ in 6-well tissue culture plates at 37 °C. When indicated, 100 ng/ml PMA, 5 mM taurine, or 100 μM resveratrol were added at the beginning of the incubation. After 1 h of incubation in the cell incubator, 50 mM DMPO was added, and the incubation was continued for 2 h more. At the end the neutrophils were collected by washing them off with $HBSS^-$ containing 1 mM EDTA ($HBSS^-$/EDTA). The supernatant and washing fluids were collected and then centrifuged to pellet the neutrophils. The A549 cell monolayers were washed once again with $HBSS^-$/EDTA to remove loosely attached cells and any remaining neutrophils. The monolayers of A549 cells were harvested by scraping, washed once with $HBSS^-$/EDTA, and packed by centrifugation ($500 \times g$). The pellets of A549 cells and neutrophils were used to extract DNA and quantify DNA-DMPO nitrone adducts. The neutrophil purity (>95% purity) and remaining neutrophils bound to A549 monolayers (<1%) were determined by analysis of a Diff-Quick staining of cytospin slides and monolayers, respectively.

*Quantification of Double-stranded DNA Bound to Microtiter Plates*—To quantify dsDNA bound to black-microplates we used 4,6-diamino-2-phenylindole (Invitrogen), which intercalates DNA and fluoresces ($\lambda_{ex}$ = 345 nm/$\lambda_{em}$ = 458 nm). Briefly, 50 μl of the reaction mixture was mixed with an equal volume of Reacti-Bind DNA coating solution (Pierce), and the plate was incubated at 37 °C for 90 min. Then the plate was washed 3 times with washing buffer (see above), and 50 μl of a

solution of 5 $\mu$M 4,6-diamino-2-phenylindole in 10 mM NaP buffer, pH 7.4, was added. After 10 min of incubation at 37 °C the fluorescence was read. Solutions of known concentrations of calf thymus dsDNA were used to prepare a calibration curve to quantify the amount of sample dsDNA bound to the plate.

*SDS-Polyacrylamide Gel Electrophoresis and Western Blot*—HL-60 or RAW 264.7 cells were washed with HBSS⁻, and cell homogenates were prepared in radioimmune precipitation assay buffer. After centrifugation at 11,700 × $g$ and 4 °C for 10 min, the supernatant was collected. The protein concentration in the supernatant was measured using a BCA protein determination kit (Pierce). Ten $\mu$l of the supernatant containing 2.5 mg of proteins/ml was separated on a 4–12% Tris-Bis Novex gel (Invitrogen), blotted onto a nitrocellulose membrane, and incubated with the rabbit anti-DMPO antiserum as recently described (11). The Western blot analysis of MPO in homogenates of RAW 264.7 cells activated with LPS was performed using an anti-human MPO antiserum that cross-reacts with murine MPO obtained from Athens Research Technology. Images were acquired from gels or Western blots developed with enhanced chemiluminescence (ECL) using a FluorChem HD2 imager (AlfaInnotech, San Leandro, CA).

*Statistical Analysis*—Relative light units (RLU) or RLU/$\mu$g of dsDNA are reported as the mean values ± S.E. Differences between pairs were determined by Student's $t$ test and between treatments and control by one-way analysis of variance with Dunnett's post hoc testing. Differences were considered statistically significant at $p < 0.05$.

## RESULTS

*HOCl Produces DNA-centered Radicals That Are Prevented by Resveratrol*—DNA nitrone adducts were produced by incubating 5 $\mu$M (as bases) calf-thymus DNA with a 2-fold molar excess of HOCl and DMPO (Fig. 1A). The omission of any of the components in the reaction mixture (*i.e.* DNA, HOCl, or DMPO) resulted in no nitrone adduct formation. Increasing the concentration of HOCl in the reaction mixture produced a corresponding increase in the formation of nitrone adducts (Fig. 1B). Although a molar ratio of one to one between DNA and HOCl produced significant formation of nitrone adducts as measured by ELISA, in subsequent experiments we used a molar ratio of two to one (DNA/HOCl) because this ratio produced higher signals than a one-to-one ratio and, thus, facilitated comparisons between treatments. The yield of nitrone adducts increased with increasing concentrations of DMPO (Fig. 1C). It is important to note that the concentration of HOCl found in sites of neutrophilic inflammation has been estimated at between 30 and 200 $\mu$M (2), which is higher than the concentrations we used in this study.

HOCl has been previously determined to react with amines in the purine and pyrimidine bases of the DNA to form chloramines, which decompose to form DNA-centered radicals (8) (Fig. 2A, *upper panel*). However, one of the most important issues regarding the use of DMPO in systems containing HOCl is the possibility that DMPO may react directly with HOCl to produce 5,5-dimethyl-2-pyrroline-*N*-oxyl radical (22), which may bind to the DNA by simple nucleophilic addition. We therefore reasoned that this adduct might potentially be detect-
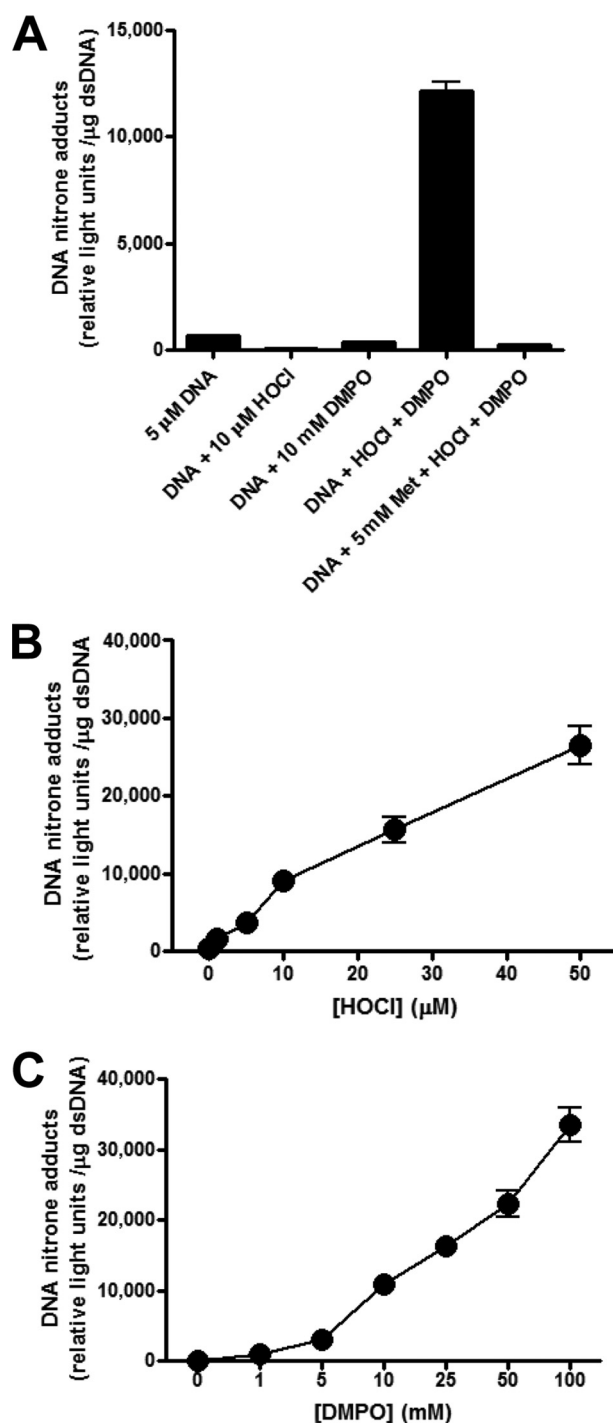


FIGURE 1. **HOCl-induces DNA-centered radicals that are trapped by DMPO to form nitrone adducts.** A, control experiments in the analysis of calf thymus DNA-DMPO nitrone adducts show the absolute requirement of DNA, HOCl, and DMPO. B and C, shown is HOCl- and DMPO-dependent, respectively, formation of calf thymus DNA-DMPO nitrone adducts. Data are shown as the mean values of relative light units/$\mu$g of dsDNA ± S.E.; $n = 9$. See "Experimental Procedures" for further details.

able using the anti-DMPO antibody. We observed that when DMPO was added 5 or 15 min after the addition of HOCl, the yield of nitrone adducts was similar, but when we added DMPO simultaneously or immediately after HOCl, the yield of nitrone adducts was reduced by ~60% (Fig. 2A, *lower panel*). When the spin trap was added 60 min after the HOCl, the yield of DNA
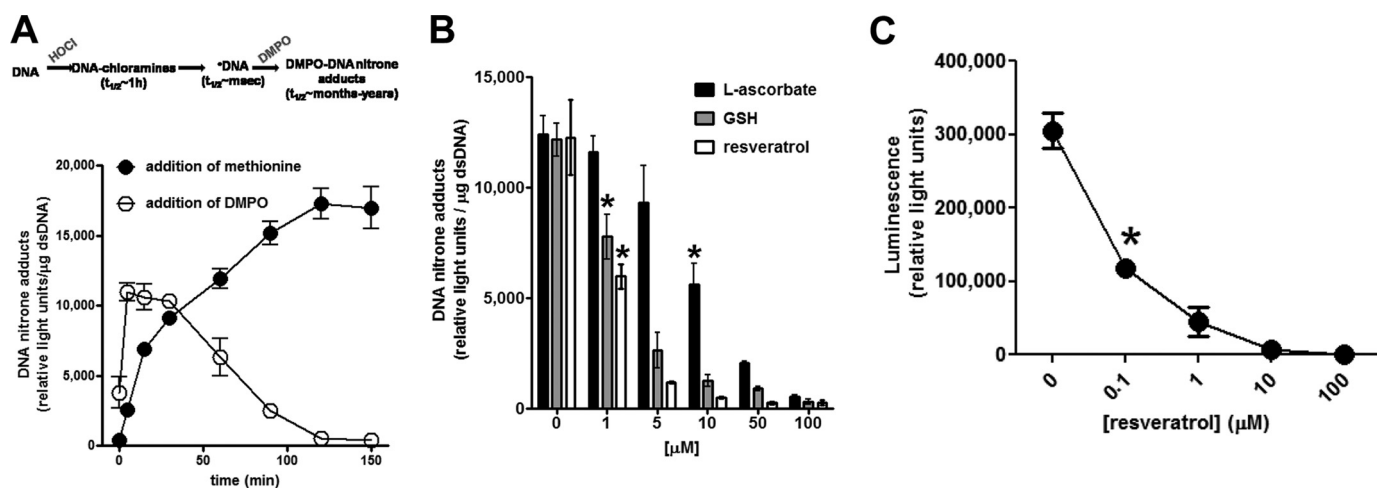
FIGURE 2. **Kinetics and effects of antioxidants on HOCl-induced DNA-DMPO nitrone adducts.** *A*, shown is the effect of time of addition of 1 mM methionine and 10 mM DMPO on the yield of nitrone adducts. The *upper panel* shows the sequence of events and half-life ($t_{1/2}$) of intermediate species, *i.e.* chloramines and DNA-centered radicals (˙DNA), produced during HOCl-triggered oxidation of DNA. *B*, shown are the concentration-dependent effects of GSH, L-ascorbate, and resveratrol on the production and trapping of HOCl-produced DNA-centered radicals with DMPO. *C*, shown is the scavenging effect of resveratrol on HOCl as assessed with luminol as a probe. *Asterisks* in *B* and *C* indicate the lowest doses of compound that produce significant ($p < 0.05$) diminution of nitrone adducts with respect to the compound not added . Data are shown as the mean values of relative light units/$\mu$g of dsDNA $\pm$ S.E.; $n = 9$.
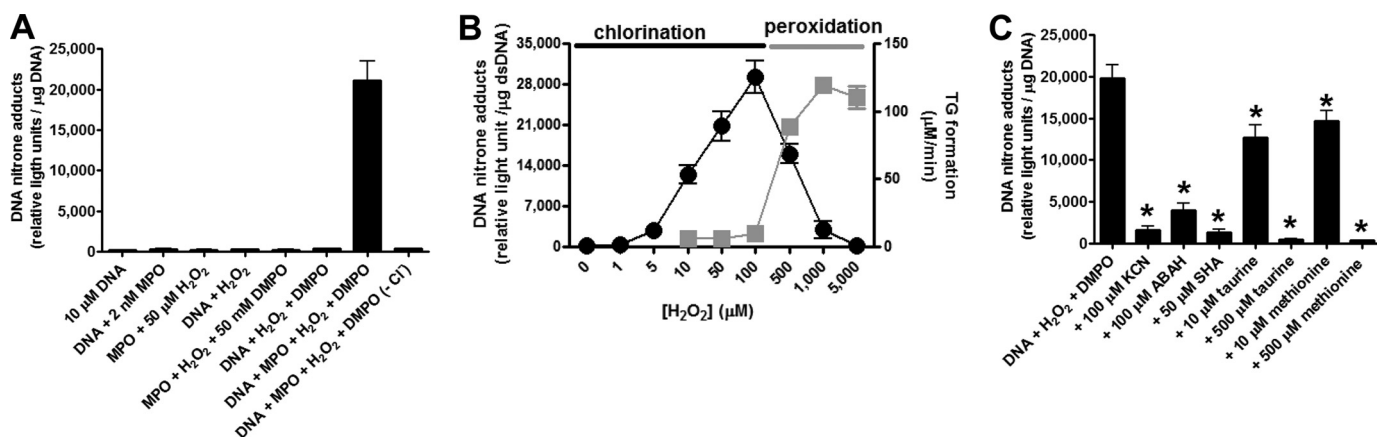


FIGURE 3. **Myeloperoxidase-driven, DNA-centered radicals, and the protective effect of resveratrol.** *A*, control experiments show the absolute need of all components, *i.e.* calf thymus DNA, active MPO, chloride, $H_2O_2$, and DMPO, to generate and trap DNA-centered radicals as assessed by ELISA. *B*, shown is the effect of $H_2O_2$ concentration on MPO-driven DNA-DMPO nitrone adduct yield and tetraguaiacol (*TG*) formation. *C*, procedures were as in *A*, but we added the MPO inhibitors and scavengers of HOCl before $H_2O_2$; the *asterisk* indicates $p < 0.05$ with respect to no inhibitor added. Data are shown as the mean values of relative light units/$\mu$g of dsDNA $\pm$ S.E.; $n = 9$. *SHA*, salicyl hydroxamic acid.

nitrone adducts decreased by ~50%, and if added 2 h after HOCl when the chloramines and their DNA radicals had already decayed, no nitrone adducts were formed (Fig. 2*A*). In addition, stopping the reaction with methionine at different times resulted in the time-dependent formation of nitrone adducts (Fig. 2*A*); however, we did not observe any further nitrone adduct formation when methionine was added 2 h after the start of the reaction. Our observations are in agreement with the kinetics of the spin trapping technique (23) and also the reported kinetics of chloramine decay (8).

Organisms have developed efficient antioxidant systems that protect their biomolecules from oxidative attacks occurring during aerobic metabolism. Two of these systems are GSH and L-ascorbate. The addition of 1 $\mu$M GSH decreased the yield of HOCl-induced DNA nitrone adducts by ~40%; thus, physiological concentrations of GSH in the cytosol of mammalian cells (*i.e.* 4 mM) (24) should be sufficient to protect genomic DNA against HOCl-triggered oxidation (Fig. 2*B*). At the same

molar concentration, GSH was more effective than L-ascorbate in reducing the yield of HOCl-triggered DNA-centered radicals *in vitro* (Fig. 2*B*). This increased efficiency was expected because of the relative rates of reaction of GSH and L-ascorbate with HOCl ($3 \times 10^7$ and $6 \times 10^6$ M$^{-1}$ s$^{-1}$ at pH 7.4, respectively) (25, 26) and possibly because of the stoichiometry (which is HOCl:L-ascorbate = 1 and HOCl:GSH = 0.5–4, depending upon the efficiency of oxidation of GSH through GSSG eventually to the chloramine derivative of the sulfonate GSO$_3^-$) (19, 27). 1 $\mu$M resveratrol reduced HOCl-induced nitrone adducts by ~50%, and at 10 $\mu$M, it completely prevented their formation (Fig. 2*B*). Resveratrol could cause this reduction either by scavenging HOCl or reacting with DNA-centered radicals before trapping with DMPO. Thus, we used a luminol-based assay to examine the reaction of resveratrol with HOCl (Fig. 2*C*). 1 $\mu$M resveratrol decreased HOCl-induced luminescence by ~90%, suggesting that it might be a potent HOCl scavenger.

*The Chlorinating Cycle of MPO Produces DNA-centered Radicals*—We hypothesized that the chlorinating cycle of MPO produces DNA-centered radicals. As shown in Fig. 3*A*, the addition of 50 $\mu$M $H_2O_2$ to a biochemical system containing calf-thymus DNA, human MPO, and $Cl^-$ was sufficient to allow us to trap DNA-centered radicals with DMPO. Omission of one or more components in this system blocked the formation of DNA nitrone adducts (Fig. 3*A*).

To distinguish the effects of chlorination *versus* peroxidation by MPO on DNA-centered radical formation, we incubated calf thymus DNA with 2 nM MPO, 100 mM $Cl^-$ (normal extracellular concentration), and different concentrations of $H_2O_2$ added as a bolus. We observed an increase in DNA-DMPO nitrone adduct formation at concentrations of $H_2O_2$ up to 100 $\mu$M (Fig. 3*B*). At higher concentrations of $H_2O_2$, the nitrone adduct yield was reduced in a concentration-dependent manner (Fig. 3*B*). Interestingly, the peroxidase activity of MPO, as assessed by the assay of oxidation of guaiacol to tetraguaiacol, was near 100% when the production of nitrone adducts decreased by 90%, *i.e.* 1 mM $H_2O_2$. DNA-DMPO nitrone adducts were blocked by inhibition of the MPO (28) with KCN, salicyl hydroxamic acid (SHA), or ABAH. Formation of adducts was also blocked by adding catalase (which decomposes $H_2O_2$; data not shown) or by scavenging HOCl with methionine or taurine (19) (Fig. 3*C*). These observations suggest that DNA-centered radicals are produced by HOCl generated during the chlorination cycle of MPO.

*The Chlorination Activity of MPO Produces DNA-centered Radicals in HL-60 Cells Exposed to $H_2O_2$*—Like neutrophils, HL-60 cells express MPO at high levels, and most of this is located in the cell nuclei (29). We therefore used HL-60 cells exposed to $H_2O_2$ and DMPO to study genomic DNA-centered radicals in a process driven by MPO and triggered by HOCl. To better model the inflammatory scenario, we triggered the chlorination cycle of MPO in the cell nuclei by two different methods: we either added low concentrations of $H_2O_2$ to the medium or incubated the cells in $HBSS^-$ with 5.6 mM glucose and 100 mM chloride, initiating the production of $H_2O_2$ by adding GO. We added DMPO 30 min after the addition of GO, when measurable amounts of HOCl had formed and reacted with DNA but DNA-chloramines had not yet decayed. The generation of $H_2O_2$ by the glucose/GO system at 30 nmol/min produced nitrone adducts inside of the cell without significant cell death (Fig. 4*A*). Catalase, cyanide, ABAH, and resveratrol inhibited the formation of DNA-centered radicals inside HL-60 cells. This occurred whether or not the cells were incubated with a bolus of $H_2O_2$ or subjected to generation of $H_2O_2$ by glucose/GO (data not shown, see also Fig. 4*A*). Because myeloid cells contain high concentrations of GSH (~4 mM) (24), ascorbate (1–4 mM) (30), taurine (~50 mM) (28), and peroxide-degrading enzymes such as catalase and glutathione peroxidase, the amount of $H_2O_2$ required to trigger HOCl production by MPO and formation of DNA-centered radicals is higher than that required to produce HOCl in the biochemical system (*i.e.* MPO/$Cl^-$/$H_2O_2$, see Figs. 3, *A*–*C*).

The 5.6 mM glucose, 1 milli-IU/ml GO system, which produced 30 nmol of $H_2O_2$/min, not only produced the highest level of DNA nitrone adducts but is also perhaps more physio-

logically relevant than the bolus addition of $H_2O_2$. As shown in Fig. 4*B*, concentrations of GO used in the present study produced a minimal loss of cell viability as assessed by the trypan blue exclusion assay. However, 5 milli-IU/ml GO produced significant cell death. We also quantified the nitrone adduct formation after washing the cells and extracting the DNA (Fig. 4*B*, right axis). We observed a GO-dependent, therefore $H_2O_2$-dependent, increase in the formation of DNA-centered radicals, whereas heat-inactivated GO did not produce nitrone adducts (data not shown). These results suggest that DNA-centered radicals are produced inside living cells and may be involved in the death of neutrophils at sites of inflammation. Although we have established an effective procedure to isolate the DNA that avoids further radical oxidation and was free of proteins (18), we sought to investigate whether protein-centered radicals such as histone-DMPO nitrone adducts are also formed. Interestingly, we detected no protein-DMPO nitrone adducts as assessed by Western blot of the HL-60 cell homogenate using the antibody anti-DMPO (Fig. 4*C*). Light bands and smears observed in the *right panel* of Fig. 4*C* may be due to adsorption to proteins of DNA nitrone adducts partially hydrolyzed with the Benzonase™ we used in the radioimmune precipitation assay buffer to prepare the cell homogenates.

To localize DNA-centered radicals inside HL-60 cells treated with $H_2O_2$ and $Cl^-$, we exposed cells under conditions in which cell viability was higher than 85%, *i.e.* glucose/GO (1 milli-IU/ml), and in which the cell viability was compromised, *i.e.* 5 milli-IU GO/glucose (see Fig. 4*B*). The analysis of these cells showed co-localization of DNA and DNA-DMPO nitrone adducts in the cell nuclei. Preincubation of the HL-60 cells with resveratrol prevented the formation of GO-induced DNA-DMPO nitrone adducts (data not shown). As shown in Fig. 4*D* and *insets*, all of the nitrone adduct formation was associated with the DNA, which we suggest is due to the proximity of the genomic DNA to the source of HOCl (*i.e.* the chlorinating cycle of MPO). The pattern of the nuclear distribution of nitrone adducts and DNA observed with 5 milli-IU GO may be related to chromatin condensation due to apoptosis (Fig. 4*D*, *right panel*). Importantly, about 90% of the cells showed nitrone adduct formation. Taken together these results indicate that DMPO traps MPO-driven, HOCl-triggered DNA-centered radicals that were formed in a cell system where molecular targets co-localized with the source of reactive chemical species. This cell model may represent reactions that occur in the nuclei of activated neutrophils and macrophages at the site of inflammation.

*DNA-centered Radicals Induced by Newly Synthesized and Uptaken MPO and the Protective Role of Resveratrol*—We used two models to simulate the induction of MPO in activated macrophages and the uptake of neutrophil-derived extracellular MPO by epithelial cells, as occurs for example in the inflamed lung (31). The first model uses RAW 264.7 macrophages activated with bacterial LPS, to induce the synthesis of MPO (Fig. 5*A*, *upper panel*). We activated the LPS-elicited macrophages with PMA to induce NADPH oxidase-2 coupling to the cell membrane and to $O_2^-$ production followed 1 h later by the addition of 50 mM DMPO. When we extracted the DNA from these macrophages, we observed nitrone adducts only in
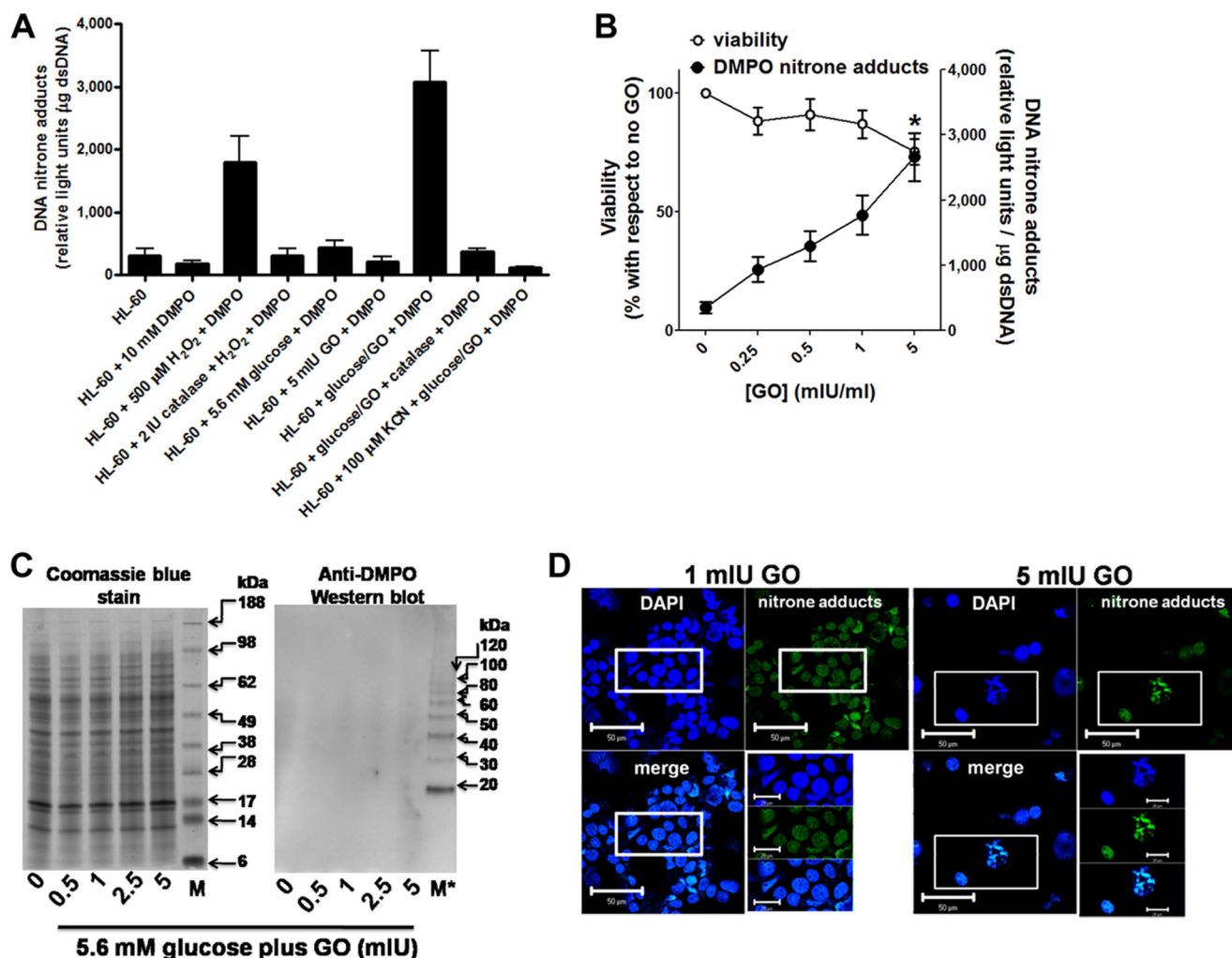
FIGURE 4. **DNA-centered radicals in HL-60 cell treated with $H_2O_2$.** *A*, shown is ELISA analysis of DNA-nitrone adducts in DNA extracted and purified from HL-60 cells that we treated with $H_2O_2$ added as a bolus or generated by glucose/GO system. We started the reaction with GO and 30 min later we added DMPO. *B*, shown is generation and trapping of DNA-centered radicals with DMPO and viability of HL-60 exposed to different fluxes of $H_2O_2$ produced by the glucose/GO system. The *asterisk* indicates changes ($p < 0.05$) in cell viability with respect to no GO added. *C*, *Coomassie blue* stain (*left panel*) and anti-DMPO Western blot (*right panel*) of homogenates of HL-60 cells that we treated as described in *B* are shown. *M* and *M\** indicate SeeBlue™ and Magic Mark™ XP molecular weight markers, respectively. *D*, shown is confocal microscopy analysis of nitrone adducts inside HL-60 cells that we incubated with 5.6 mM glucose and 1 or 5 milli-IU of GO and 10 mM DMPO. The measurement *bar* is 50 μm. *Insets* show nuclear DNA, nitrone adducts, and merge images from individual cells treated as in the main panel, and the *bar* indicates 20 μm. Data is from at least three experiments performed in triplicate, and they show a representative image or mean values of relative light units/μg of dsDNA ± S.E.; $n = 9$. See "Experimental Procedures" for further details. *DAPI*, 4′,6-diamidino-2-phenylindole.

those macrophages preincubated with LPS and activated with PMA (Fig. 5*A*, *lower panel*). PMA-triggered DNA-DMPO nitrone adducts were prevented with diphenylene iodonium and apocynin, two inhibitors of NADPH oxidase-2 (32). Salicyl hydroxamic acid and ABAH are two known inhibitors of MPO activity (28). Nitrone adduct formation was also prevented by addition of resveratrol but not taurine or methionine (Fig. 5*B*). This result might indicate that resveratrol passes more easily across cell membranes than the charged taurine or methionine.

The second model uses A549 cells preloaded with human MPO exposed to $H_2O_2$ and DMPO. When we incubated A549 lung type-2 epithelial cells with human MPO and analyzed its subcellular localization (Fig. 6*A*), we observed that most of the MPO was localized to the perinuclear region of the cells (Fig. 6*A, lower panel*). When we treated these cells with glucose/GO to generate $H_2O_2$ and activated the chlorination cycle of MPO, we observed the formation of nitrone adducts with no signifi-

cant change in cell viability (Fig. 6*B*). In this model resveratrol also prevented nitrone adduct formation (Fig. 6*C*). Fig. 6*D* shows that PMA activation induces DNA-centered radicals in A549 cells co-cultured with neutrophils. We also observed a small amount of DNA-centered radicals in PMA-activated neutrophils. The aim of these experiments was to test whether genomic DNA radicals in A549 cell monolayers were produced by HOCl that escapes from PMA-activated neutrophils, HOCl produced by extracellular MPO, or HOCl produced intracellularly by MPO that was taken up by A549 cells. Interestingly, resveratrol, but not taurine, blocked DNA-centered radical formation in neutrophils and A549 cells co-incubated with neutrophils (Fig. 6*D*). Similar results were obtained when these experiments were performed in complete culture medium (data not shown). Results using this model indicated that resveratrol passes through cell membranes and scavenges HOCl, consequently blocking DNA-centered radical formation.
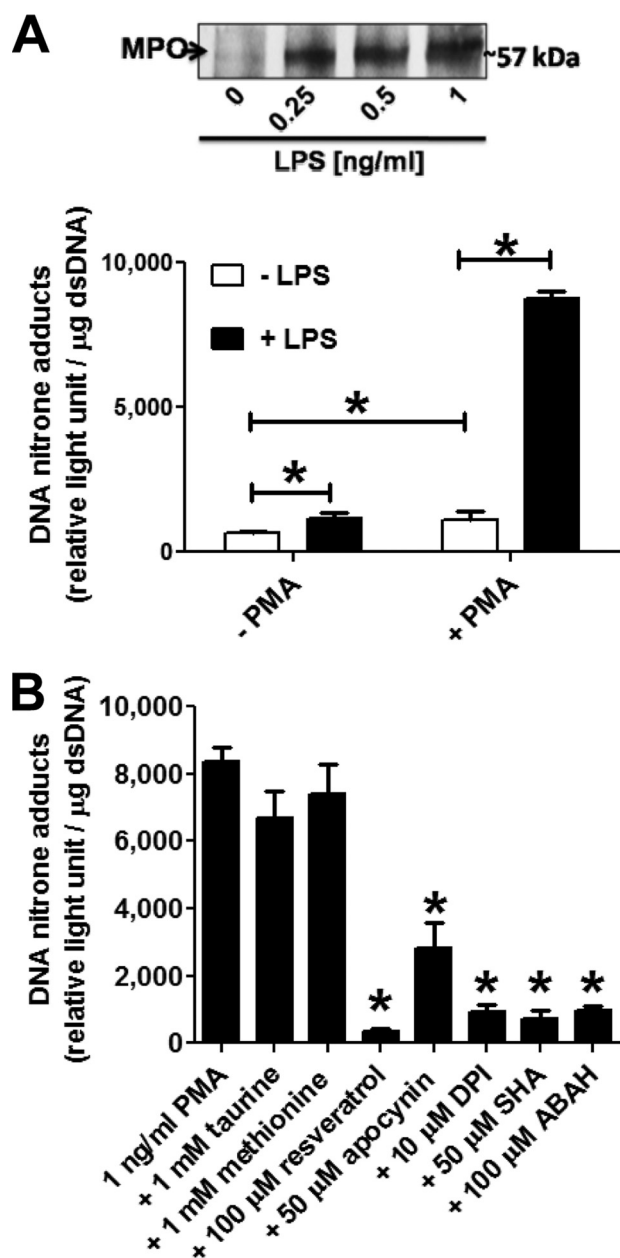
FIGURE 5. **Critical role of MPO on DNA-centered radical production in macrophages stimulated with LPS when activated with PMA.** *A*, in the *upper panel* we show a Western blot analysis of MPO in macrophages treated for 24 h with different concentrations of bacterial LPS. In the *lower panel* we show the yield of nitrone adducts in the DNA purified from macrophages treated with 1 ng/ml LPS for 24 h and then activated for 1 h with the phorbol ester PMA (1 ng/ml). Then 50 mM DMPO was added, and the incubation was continued for 1 h before extraction of DNA. *Asterisks* indicate that means connected by the horizontal segments are different ($p < 0.05$). *B*, we induced MPO in RAW 264.7 cells, then added different compounds (inhibitors and scavengers) and activated the cells with PMA. We trapped DNA-centered radicals with 50 mM DMPO and analyzed nitrone adducts by ELISA. The *asterisk* indicates significant difference with respect to PMA alone. Data are from at least three experiments performed in triplicate, and they show a representative image or mean values of relative light units/$\mu$g of dsDNA $\pm$ S.E.; $n = 9$. *SHA*, salicyl hydroxamic acid; *DPI*, diphenylene iodonium.

## DISCUSSION

In these studies we tested the hypothesis that intracellular MPO produces DNA-centered radicals in *in vitro* models of inflammation. The formation of DNA-centered radicals involves the formation of chloramines that decompose to form

DNA-centered radicals that are trapped by DMPO. To test our hypothesis we investigated HOCl-induced DNA-centered radicals in biochemical and cell models and analyzed their inhibition by resveratrol (summarized in Scheme 1). Previously we reported the formation of DNA-DMPO nitrone adducts by attack of genomic DNA by $^{\bullet}$OH radicals produced by a Fenton-like system, *i.e.* the $Cu^{2+}/H_2O_2$ system (33). However, the chemistry of the reaction of DNA with HOCl differs from that of $^{\bullet}$OH in a number of ways. HOCl is less reactive than $^{\bullet}$OH and, thus, can diffuse greater distances than $^{\bullet}$OH (34). It also reacts rapidly with amino and sulfhydryl groups in proteins and with amino groups in nucleic acids (34, 35). In addition, it reacts rapidly with lipids, carbohydrates, GSH, taurine, methionine, and L-ascorbate (19, 36). Consequently, because of HOCl reactivity and the presence of cellular antioxidants, oxidation of genomic DNA by HOCl might occur only when HOCl is produced close to or within the cell nuclei. DNA oxidation by HOCl can lead to oxidative consequences such as chlorinated bases (3), including 5-chloro-2'-deoxycytidine, 8-chloro-2'-deoxyadenine, and 8-chloro-2'-deoxyguanosine, 8-oxo-7,8-dihydro-2'-deoxyguanosine (37), abasic sites (loss of a base in DNA), strand breaks (8, 38), mutations, and carcinogenesis (39, 40).

The anti-inflammatory and anti-carcinogenic effects of resveratrol have been attributed to its properties as a scavenger of $O_2^-$ and $^{\bullet}$OH (41). In addition, resveratrol inhibits $O_2^-$ production by NADPH oxidase-2 (15), blocks cyclooxygenase activity (42), and thus, might protect DNA against mutations induced by reactive oxygen species (see Scheme 1). To test whether resveratrol inhibits HOCl-triggered DNA oxidation, we measured the ability of resveratrol to block DNA-DMPO nitrone adduct formation and luminol oxidation by HOCl. Although luminol has been recently used to image HOCl production by MPO *in vivo* (20), it is known that luminol reacts with peroxynitrite and $O_2^-$, which are also produced during inflammation (32, 43). When we treated calf thymus DNA with HOCl and DMPO, we observed that resveratrol inhibits nitrone adduct formation (Fig. 2B). However, based on our data we cannot rule out a reaction of resveratrol with the DNA-chloramines or with DNA-centered radicals once they are formed. The ability of resveratrol to block HOCl-induced luminol luminescence indicates that it reacts with HOCl, but the mechanism remains to be elucidated. In addition, the capability of resveratrol to prevent DNA-centered radical formation may be related to its anti-mutagenic and anti-carcinogenic effects, which have been observed both in animal models of inflammation and in clinical studies (Ref. 2 and references therein). In addition, a study by Hensley and Floyd (17) indicated that resveratrol inhibits the peroxidase activity of MPO. Indeed, as shown in Fig. 3B, after reaction of MPO/Cl$^-$ with 1 mM $H_2O_2$, the chlorination chemistry of MPO was almost completely blocked by resveratrol; however, the peroxidase activity was still high. Low concentrations of $H_2O_2$ are known to trigger the chlorination cycle of MPO, which produces HOCl by oxidation of chloride. Thus, resveratrol may inhibit DNA-centered radical formation by scavenging HOCl rather than inhibiting MPO activity. However, in agreement with the observations of Hensley and Floyd (17), we observed that resveratrol inhibits MPO peroxidase
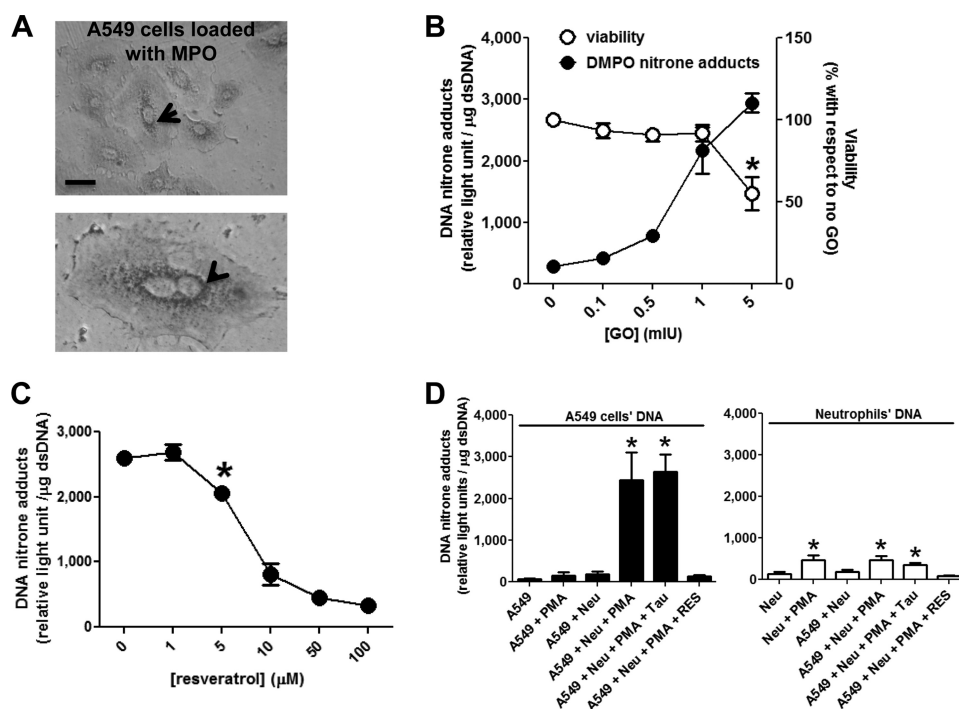
FIGURE 6. **Uptaken MPO is a source of genomic DNA-centered radicals in epithelial cells exposed to H₂O₂.** *A*, in the *upper panel* we preloaded A549 cells with 50 nM human MPO for 24 h and analyzed MPO using an anti-human MPO antibody, a secondary antibody conjugated with horseradish peroxidase, and 3,3′-diaminodbenzidine as substrate. The *black bar* indicates 10 $\mu$m, and the *arrowhead* indicates the perinuclear localization of the uptaken MPO. The *lower panel* shows the image of one representative A549 cell loaded with MPO. *B*, the procedure was the as in *A*, but we treated the pre-loaded cells with 5.6 mM glucose and different concentrations of GO. Thirty minutes later we added 50 mM DMPO. After 1 h of incubation we determined membrane trypan blue exclusion (viability), extracted DNA, and analyzed DNA-DMPO nitrone adducts by ELISA. The *asterisk* indicates changes ($p < 0.05$) in cell viability with respect to the cell viability without GO added. *C*, procedures were as in *B*, but we incubated pre-loaded A549 cells at 37 °C for 1 h with the indicated concentrations of resveratrol in HBSS⁺ with 5.6 mM glucose and started the formation of H₂O₂ by adding 1 milli-IU GO. Thirty minutes later we added 50 mM DMPO and continued the incubation for one more hour. The *asterisk* indicates the minimal concentration of resveratrol that significantly ($p < 0.05$) changes nitrone adduct production with respect to no resveratrol added. *D*, monolayers of A549 cells were incubated with or without neutrophils (*Neu*) in HBSS⁺ and with or without 100 ng/ml PMA, 100 $\mu$M resveratrol (*RES*), or 5 mM taurine (*Tau*). 1 h later 50 mM DMPO was added. After a total of 3 h of incubation the nitrone adducts were determined in the DNA extracted from both cell populations (A549 cell and neutrophil DNA) as described under "Experimental Procedures." *Asterisks* indicate $p < 0.05$ with respect to DNA nitrone adducts determined in the DNA isolated from A549 cells that were incubated with neutrophils (*A549+Neu bar*). Data are shown as the mean values of relative light units/$\mu$g of dsDNA ± S.E.; $n = 9$.

also been reported in animal models of chronic inflammation and clinical studies (Ref. 2 and references therein). Our results indicate that MPO taken up from the medium localizes in the perinuclear region of the A549 airway type-II epithelial cells (Fig. 6*A*). Type II epithelial cells are one of the most vulnerable targets for cell transformation during lung neutrophilic inflammation induced by exposure to particulate air pollutants (45). The localization of MPO near the nucleus is striking because of the proximity of the genome to the source of HOCl and suggests a possible mechanism in which MPO taken up by cells can trigger genotoxic effects in surrounding epithelial cells in inflamed tissues (45). HOCl produced during activation of neutrophils can diffuse outside the phagolysosome and react with the membrane or with other macromolecules in surrounding cells (46), which would limit its ability to react with their genomic DNA. Our results (Fig. 6*D*) indicate that the HOCl produced by MPO inside A549 cells caused DNA-centered radical formation. That taurine does not prevent DNA-centered radical formation in A549 cells incubated with activated neutrophils suggests that HOCl produced from neutrophils or produced extracellularly by released MPO is not the cause of DNA-centered radical formation in A549

activity inside HL-60 cells (data not shown). Most importantly, results from our cell models are consistent with our hypothesis that resveratrol passes through cell membranes and scavenges HOCl, consequently blocking DNA-centered radical formation (see Scheme 1).
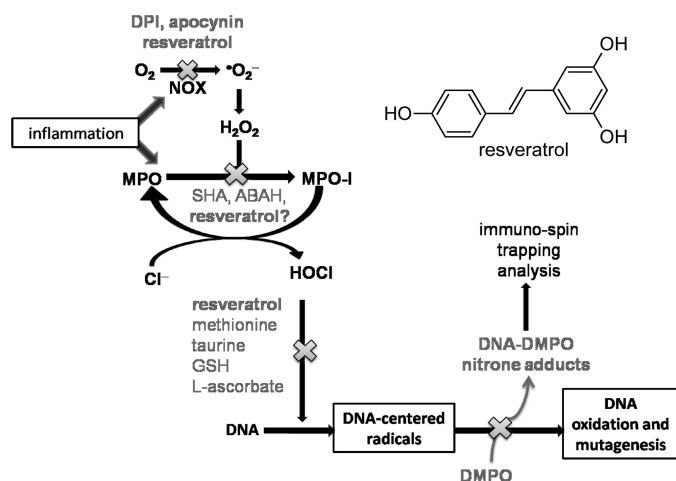
For the first time we have imaged DNA-centered radicals and observed structural changes in the nuclei of HL-60 cells exposed to H₂O₂. The close proximity between DNA and MPO in HL-60 cells and possibly in activated neutrophils (44) makes these cells particularly vulnerable to oxidative damage to their genomes and subsequent cell death. To protect the genome while at sites of inflammation, neutrophils contain high concentrations of L-ascorbate, GSH, and taurine. Our results indicate that these scavengers can protect against HOCl-triggered DNA-centered radicals (see Scheme 1).

It is known that activation of neutrophils and inflammatory macrophages with PMA produces mutations in phagocytized bacteria, and it transforms mammalian cells (2, 39). Furthermore, tumor development in sites of neutrophil infiltration has

cells. On the other hand, resveratrol that diffuses inside the cell and scavenges HOCl can prevent DNA oxidation in cells that took up MPO released from PMA-activated neutrophils. It is important to note that at sites of inflammation, the concentrations of H₂O₂ have been reported to reach ∼50–100 $\mu$M (7), sufficient to trigger the chlorination cycle of MPO (5). In addition, H₂O₂ is very stable and can cross cell membranes and be used as substrate by MPO located close to the DNA, producing HOCl and damage to the genome. Taken together, our study suggests that DNA-centered radicals participate early in inflammation-induced carcinogenesis. Therefore, inhibitors of the chlorination cycle of MPO, scavengers of HOCl, and spin traps might all be useful for stopping early DNA oxidation, mutagenesis, and cell transformation in sites of inflammation.

We conclude that in the site of inflammation, the genomes of both inflammatory and surrounding epithelial cells are targets of HOCl generated intracellularly by MPO, both newly synthesized and that taken up from the inflammatory milieu. In addition, this is the first report showing the formation of HOCl-

**SCHEME 1. MPO chlorinating activity and DNA-centered radicals in the pathway from inflammation to carcinogenesis.** Inflammation induces increased membrane coupling and activity of NADPH oxidase (*NOX*) and recruitment and activation of neutrophils that release MPO. Active NADPH oxidase reduces dioxygen to superoxide radical anion ($O_2^-$) that spontaneously or enzymatically dismutates to $H_2O_2$. NADPH oxidase can be inhibited with apocynin, diphenylene iodonium (*DPI*), and resveratrol. $H_2O_2$ is used by MPO to oxidize chloride to hypochlorous acid (HOCl). This reaction is inhibited by salicyl hydroxamic acid (*SHA*) or ABAH. HOCl reacts with DNA to form chloramines that decompose to produce DNA-centered radicals. HOCl is scavenged by taurine, methionine, reduced glutathione (GSH), L-ascorbate, and possibly by resveratrol (chemical structure shown in the *inset*). Once formed and if not scavenged by antioxidants or trapped by DMPO to form a nitrone adduct, DNA-centered radicals can lead to oxidation of the DNA, mutations, and cell transformation. *Crosses* indicate inhibition or scavenging. See "Results" and "Discussion" for further details.

induced genomic DNA-centered radicals in living cells and suggests a mechanism for the anti-carcinogenic effect of resveratrol. Finally, our findings provide biochemical bases of early events of HOCl-induced genomic instability that may provide new therapeutic strategies to block inflammation-induced carcinogenesis.

## REFERENCES

1. Weitzman, S. A., Weitberg, A. B., Clark, E. P., and Stossel, T. P. (1985) *Science* **227,** 1231–1233
2. Weitzman, S. A., and Gordon, L. I. (1990) *Blood* **76,** 655–663
3. Ohshima, H., Tatemichi, M., and Sawa, T. (2003) *Arch. Biochem. Biophys.* **417,** 3–11
4. Klebanoff, S. J. (1970) *Science* **169,** 1095–1097
5. Dunford, H. B. (1999) in *Heme Peroxidases* (Dunford, H. B. ed) pp. 349–378, John Wiley & Sons, Inc., New York
6. Nauseef, W. M., Metcalf, J. A., and Root, R. K. (1983) *Blood* **61,** 483–492
7. Cerutti, P. A., and Trump, B. F. (1991) *Cancer Cells* **3,** 1–7
8. Hawkins, C. L., and Davies, M. J. (2002) *Chem. Res. Toxicol.* **15,** 83–92
9. Pattison, D. I., Davies, M. J., and Asmus, K. D. (2002) *J. Chem. Soc. Perkin Trans.* **2,** 1461–1467
10. Mason, R. P. (2004) *Free Radic. Biol. Med.* **36,** 1214–1223
11. Gomez-Mejiba, S. E., Zhai, Z., Akram, H., Deterding, L. J., Hensley, K., Smith, N., Towner, R. A., Tomer, K. B., Mason, R. P., and Ramirez, D. C. (2009) *Free Radic. Biol. Med.* **46,** 853–865
12. Athar, M., Back, J. H., Tang, X., Kim, K. H., Kopelovich, L., Bickers, D. R., and Kim, A. L. (2007) *Toxicol. Appl. Pharmacol.* **224,** 274–283
13. Cheson, B. D. (2009) *Clin. Adv. Hematol. Oncol.* **7,** 142
14. Sengottuvelan, M., Deeptha, K., and Nalini, N. (2009) *Chem. Biol. Interact.* **181,** 193–201
15. Park, D. W., Baek, K., Kim, J. R., Lee, J. J., Ryu, S. H., Chin, B. R., and Baek, S. H. (2009) *Exp. Mol. Med.* **41,** 171–179
16. Birrell, M. A., McCluskie, K., Wong, S., Donnelly, L. E., Barnes, P. J., and Belvisi, M. G. (2005) *FASEB J.* **19,** 840–841
17. Hensley, K. L., and Floyd, R. A. (November 25, 1999) World Intellectual Property Organization Patent WO/1999/059561
18. Ramirez, D. C., Gomez-Mejiba, S. E., and Mason, R. P. (2007) *Nat. Protoc.* **2,** 512–522
19. Prütz, W. A. (1996) *Arch. Biochem. Biophys.* **332,** 110–120
20. Gross, S., Gammon, S. T., Moss, B. L., Rauch, D., Harding, J., Heinecke, J. W., Ratner, L., and Piwnica-Worms, D. (2009) *Nat. Med.* **15,** 455–461
21. Nauseef, W. M. (2007) *Methods Mol. Biol.* **412,** 15–20
22. Bernofsky, C., Bandara, B. M., and Hinojosa, O. (1990) *Free Radic. Biol. Med.* **8,** 231–239
23. Janzen, E. G. (1984) *Methods Enzymol.* **105,** 188–198
24. Bilzer, M., and Lauterburg, B. H. (1991) *Eur. J. Clin. Invest.* **21,** 316–322
25. Pattison, D. I., and Davies, M. J. (2001) *Chem. Res. Toxicol.* **14,** 1453–1464
26. Folkes, L. K., Candeias, L. P., and Wardman, P. (1995) *Arch. Biochem. Biophys.* **323,** 120–126
27. Nagy, P., and Ashby, M. T. (2007) *Chem. Res. Toxicol.* **20,** 79–87
28. Malle, E., Furtmüller, P. G., Sattler, W., and Obinger, C. (2007) *Br. J. Pharmacol.* **152,** 838–854
29. Murao, S., Stevens, F. J., Ito, A., and Huberman, E. (1988) *Proc. Natl. Acad. Sci. U.S.A.* **85,** 1232–1236
30. Washko, P., Rotrosen, D., and Levine, M. (1989) *J. Biol. Chem.* **264,** 18996–19002
31. Knaapen, A. M., Güngör, N., Schins, R. P., Borm, P. J., and Van Schooten, F. J. (2006) *Mutagenesis* **21,** 225–236
32. Lambeth, J. D. (2004) *Nat. Rev. Immunol.* **4,** 181–189
33. Ramirez, D. C., Mejiba, S. E., and Mason, R. P. (2006) *Nat. Methods* **3,** 123–127
34. Winterbourn, C. C. (2008) *Nat. Chem. Biol.* **4,** 278–286
35. Winterbourn, C. C. (2002) *Toxicology* **181–182,** 223–227
36. Pattison, D. I., and Davies, M. J. (2006) *Curr. Med. Chem.* **13,** 3271–3290
37. Shen, Z., Wu, W., and Hazen, S. L. (2000) *Biochemistry* **39,** 5474–5482
38. Cadet, J., Douki, T., Gasparutto, D., and Ravanat, J. L. (2003) *Mutat. Res.* **531,** 5–23
39. Weitzman, S. A., and Stossel, T. P. (1981) *Science* **212,** 546–547
40. Güngör, N., Knaapen, A. M., Munnia, A., Peluso, M., Haenen, G. R., Chiu, R. K., Godschalk, R. W., and van Schooten, F. J. (2010) *Mutagenesis* **25,** 149–154
41. Leonard, S. S., Xia, C., Jiang, B. H., Stinefelt, B., Klandorf, H., Harris, G. K., and Shi, X. (2003) *Biochem. Biophys. Res. Commun.* **309,** 1017–1026
42. Szewczuk, L. M., Forti, L., Stivala, L. A., and Penning, T. M. (2004) *J. Biol. Chem.* **279,** 22727–22737
43. Babior, B. M. (1988) *Hematol. Oncol. Clin. North Am.* **2,** 201–212
44. Brinkmann, V., Reichard, U., Goosmann, C., Fauler, B., Uhlemann, Y., Weiss, D. S., Weinrauch, Y., and Zychlinsky, A. (2004) *Science* **303,** 1532–1535
45. Knaapen, A. M., Seiler, F., Schilderman, P. A., Nehls, P., Bruch, J., Schins, R. P., and Borm, P. J. (1999) *Free Radic. Biol. Med.* **27,** 234–240
46. Pullar, J. M., Vissers, M. C., and Winterbourn, C. C. (2000) *IUBMB Life* **50,** 259–266